Achieving Superconductivity with Higher T_c in Lightweight Al-Ti-Mg Alloys: Prediction using Machine Learning and Synthesis via High-Pressure Torsion Process

Masaki Mito[1],* Narimichi Mokutani[1], Hiroki Tsuji[1], Yongpeng Tang[1], Kaname Matsumoto[1], Mitsuhiro Murayama[2,3], and Zenji Horita[1,4,5]
[1] *Graduate School of Engineering, Kyushu Institute of Technology, Kitakyushu 804-8550, Japan*
[2] *Department of Materials Science and Engineering, Virginia Polytechnic Institute and State University, Blacksburg, VA 24061, USA*
[3] *Institute for Materials Chemistry and Engineering, Kyushu University, Kasuga 816-8580, Japan*
[4] *Magnesium Research Center, Kumamoto University, Kumamoto, 860-8555 Japan and*
[5] *Synchrotron Light Application Center, Saga University, Saga 840-8502, Japan*
(Dated: January 27, 2022)

Aluminum (Al) and titanium (Ti) are superconducting materials but their superconducting transition temperatures (T_c) are quite low as 1.20 and 0.39 K, respectively, while magnesium (Mg) never exhibits superconductivity. In this study, we explored new superconductors with higher T_c in the Al-Mg-Ti ternary system, along with the prediction using machine learning. High-pressure torsion (HPT) is utilized to produce the superconducting states. While performing AC magnetization measurements, we found, for the first time, superconducting states with T_c = 4.0 and 7.3 K for a composition of Al:Ti = 1:2. The magnetic anomalies appeared more sharply when the sample was processed by HPT at 573 K than at room temperature, and the anomalies exhibited DC magnetic field dependence characteristic of superconductivity. Magnetic anomalies also appeared at ∼55 K and ∼93 K, being supported by the prediction using the machine learning for the Al-Ti-O system, and this suggests that Al-Ti oxides play an important role in the advent of such anomalies but that the addition of Mg could be less effective.

I. INTRODUCTION

Among the elements in the periodic table, 29 elements act as superconductors at ambient pressure. In addition, 24 elements become superconductors at high pressures [1, 2]. If a superconductor with a high superconducting (SC) transition temperature (T_c) could be obtained using only light metals such as Al, Ti, Mg and their alloys, the industrial impact would be significant because they are ubiquitous, eco-friendly and rather cheap metals and can be easily drawn into wires.

Al and Ti become superconductors at ambient pressure with T_c of 1.20 K and 0.39 K, respectively [3]. However, Mg does not become a superconductor even at high pressure. Any of the Al-Ti alloys does not have a T_c exceeding 1.20 K [3, 4], as seen in Table I. Most of T_c for the Al-Mg alloys are also lower than 1.20 K [3, 5–7] except for the two alloys of which T_c are 1.5 and 1.7 K [6, 8]. The Ti-oxides have T_c of less than 2.3 K [9], and most of them have T_c of less than 1.0 K [9–11]. However, in thin films on substrates, some of T_c exceed the liquid helium temperature (4.2 K) [12, 13]. This suggests that there should be a positive effect of structural strain on increasing T_c. The oxide compositions are different from 1:2 of familiar TiO_2 [12–14]. For reference, the superconductivity with T_c = 4.5 K was also observed in the Mg spinel compounds including Ti_xO_y, $MgTi_2O_4$ on substrate $SrTi_2O_3$ [15], and it can be considered as strain-induced superconductivity.

Machine learning based on the relating database may be useful to confirm T_c for actual superconductors [16] and should be helpful in exploring new superconductors [17, 18]. In this study, we explore potential superconductors using Al, Ti, and Mg with the help of the prediction by machine learning.

Let us state the first law of thermodynamics as a principle law:

$$\Delta U = \Delta Q + \Delta W, \tag{1}$$

where ΔU, ΔQ, and ΔW are the deviations in the internal energy, heat, and work, respectively. The microstructure of a material in stable and quasi-stable states is generally controlled by heat treatment through ΔQ and by plastic deformation through ΔW. In this study, we used the process of high-pressure torsion (HPT) [19, 20], which inputs significant ΔW to the materials. The operation of HPT was carried out at an elevated temperature to provide additional energy ΔQ.

It should be noted that this HPT process is applicable to high-strength and less ductile materials [21], including ceramics [22] and semiconductors to improve their prpoperties [23]. The HPT process was also employed to enhance T_c in several metallic materials, as documented in recent review papers [24, 25]. Moreover, the HPT process can consolidate powders [26, 27] and can be scaled up for the production of wires [28], large sheets, and rods [29].

*Electronic address: mitoh@mns.kyutech.ac.jp

TABLE I: T_c of Ti, Ti oxides, Al, Al-Ti alloys, Al-Mg alloys, Mg-Ti oxides, and Al-Ti oxide including sample states, references and years in publication.

chemical formula	film or not	T_c [K]	Ref.	year
Ti		0.39	[3]	1963
TiO		2.3	[9]	1968
$TiO_{1.07}$		1.0	[10]	1972
$TiO_{1.06}$		0.54	[10]	1972
$TiO_{0.95}$		0.80	[10]	1972
TiO		0.64	[10]	1972
TiO		1.06	[11]	1972
$TiO_{0.92}$		0.72	[11]	1972
$TiO_{0.86}$		0.47	[11]	1972
$TiO_{0.91}$		0.70	[11]	1972
TiO	film	7.4	[12]	2017
γ-Ti_3O_5	film	7.1	[13]	2017
Ti_4O_7	film	3.0	[13]	2017
Ti_4O_7	film	2.32	[14]	2019
Al		1.20	[3]	1963
$Ali_{0.029}Ti_{0.971}$		0.65	[4]	2000
$Ali_{0.053}Ti_{0.947}$		0.70	[4]	2000
$Ali_{0.102}Ti_{0.898}$		0.73	[4]	2000
$Al_{0.28}Mg_{0.18}$		0.84	[6]	1974
$Al_{0.39}Mg_{0.61}$		1.5	[6]	1974
$Al_{0.6}Mg_{0.4}$		1.7	[8]	1973
$Al_{0.61}Mg_{0.39}$		0.84	[6]	1974
Ali_3Ti		1.02	[3]	1963
Al_2Mg_2		0.84	[5]	1973
Al_3Mg_2		0.84	[3]	1963
Al_3Mg_2		0.87	[7]	2007
$MgTi_2O_4$	film	4.5	[15]	2020

II. MACHINE LEARNING CALCULATION

First, based on the educational materials in the database on metallic superconductors confirmed experimentally [30], ten runs of machine learning were conducted. The same dataset has already been used in another study [16]. It should be noted that the dataset on Ti includes NbTi with T_c = 9.5 K [31] and the one on Mg includes MgB_2 with T_c = 39 K [32]. Figure 1 shows the T_c mapping for the ternary Al-Ti-Mg system predicted by 10-fold cross-validation, based on the metallic superconductor dataset. The orange-red colors, representing $T_c > 7.5$ K, can be seen in the region surrounding $AlTi_3$, which is a stable intermetallic compound. Furthermore, the area inside the three-element triangle potentially represents $T_c > 6.0$ K. Here, the present 13 targeted compositions, except pure Al, Ti, and Mg, are circled in red in Fig. 1. Second, preliminary machine learning was also conducted for the Al-Ti-O system based on about 14,000 superconductor dataset of experimentally confirmed superconductors including cuprate and iron-based superconductors [30]. There, in order to avoid overfitting by machine learning, the dataset was supplemented with about 500 non-superconductors reported by Hosono *et al.* [33].

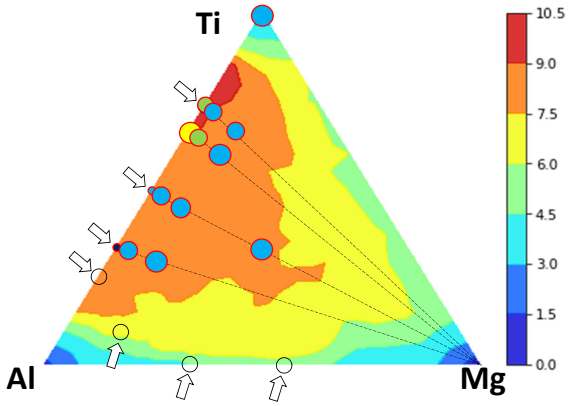

FIG. 1: (Color online) Mapping of T_c in an Al-Ti-Mg triangle, predicted by machine learning based on the metallic superconductor dataset [30]. The arrows indicate the compositions corresponding to the stable compounds (phases). The red circles represent samples prepared via the HPT processing. The observed T_c is displayed with the corresponding colors, and the magnitude of the SC shielding effects is represented by the size of the circle.

III. MATERIALS AND METHODS

Mixtures of Al, Ti and Mg powders with the purities of 99.99, 99.9, and 99.5%, respectively, were hand-pressed to disks with 10mm diameters. HPT was then conducted for the disks at room temperature under a pressure of P = 2 or 6 GPa for revolutions in the range of N = 10–1000 with a rotation speed of ω = 1 rpm. HPT was also performed at 573 K under P = 6 GPa for N = 10 with ω = 0.2 rpm (hereafter called "hot-slow HPT"). After the HPT processing, disk specimens with 4mm diameters and 0.7mm thicknesses were prepared for magnetic measurements. To examine the superconducting properties of a specimen consisting of small grains, this study used contactless magnetic measurements because they are more convenient and reliable than contact-type electrical resistance measurements especially when the specimen is superconducting. The in-phase of AC magnetization (M_{AC}') was observed as a function of temperature (T) and DC magnetic field (H_{DC}) using a commercial superconducting quantum interference device magnetometer under an AC magnetic field H_{AC} of 0.4 mT and 10 Hz (or 100 Hz). To find a diamagnetic signal along with a magnetization due to a magnetic impurity, observing M_{AC}' induced by H_{AC} at zero H_{DC} is better than observing the DC magnetization at large H_{DC}. The SC nature of the diamagnetic signal was verified via the H_{DC} dependence of M_{AC}'.

The HPT-processed samples were characterized by X-ray diffraction (XRD) analysis using monochromatic X-rays at the BL04B1 beamline of SPring-8 in JASRI. The area of the X-ray illumination was selected at 4.0 mm

away from the center of the HPT- processed disks with a size of 0.2 × 0.2 mm^2. X-ray diffraction images were recorded for a duration of 1 min with a CCD (Charge-Coupled Device) detector and were integrated and corrected for distortions using the IPAnalyzer and PDIndexer software. Details of the XRD analyses in SPring-8 were described in Ref. [34].

High resolution transmission electron microscopy (HRTEM) observations were carried out using a JEOL JEM-2100 operated at 200 kV. The microscope for this HRTEM is equipped with a JEOL 60 mm^2 silicon drift type energy dispersive X- ray detector (EDS) for chemical analysis. Thin samples for the HRTEM were prepared by mechanical thinning followed by Ar ion milling (Gatan PIPS-II) with liquid nitrogen cooling.

IV. EXPERIMENTAL RESULTS

A. XRD

Figure 2 shows the XRD pattern for the sample with the composition of Al:Ti:Mg = 1:2:0 after processing by HPT for $N = 100$ and 500 revolutions. All of identifiable peaks are due to the original ingredients, Al and α-Ti. No peaks are visible from intermetallics and other compounds within the resolution attained in this study. It should be noted that the Al peak is fairly low in comparison with the peaks of α-Ti. This indicates that the dissolution of Al in Ti proceeded due to high energy introduced by the HPT process. It is suggested that the energy state is higher than the equilibrium in consistent with earlier reports [35, 36].

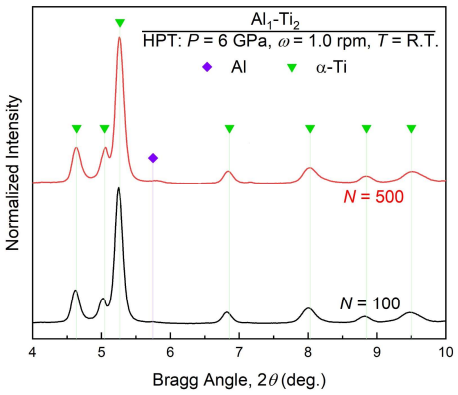

FIG. 2: (Color online) XRD pattern for Al:Ti:Mg = 1:2:0 subjected to room-temperature HPT for $N = 100$ and 500 under $P = 6$ GPa with $\omega = 1.0$ rpm. The peak positions for Al and α-Ti are marked with symbols of diamond and inverse triangle, respectively.

B. HRTEM

HRTEM images are shown in Fig. 3 from two separate regions in the HPT processed Al:Ti:Mg = 1:2:0 sample ($N = 500$). Although the dominant phase of the sample was α-Ti with dissolved Al according to the XRD analysis in Fig. 2, Fast Fourier Transform (FFT) analysis revealed that the diffractgrams from the square areas in Fig. 3(a) and (b) were identified to be $AlTi_3$ and AlTi intermetallics phases, respectively. This observation is consistent with the Al-Ti binary phase diagram that the composition of Al:Ti:Mg = 1:2:0 lies in the $AlTi_3$ and AlTi two-phase region. It is considered that a solid-state reaction occurred due to a high energy state produced by the HPT process as reported earlier [26, 27]. It should be noted that such intermetallics are not superconducting (SC) according to the literatures in Table I. Thus, as discussed later, the SC state found in this alloy should be attributed to some other phases that were are not detected in the present XRD and HRTEM analyses.

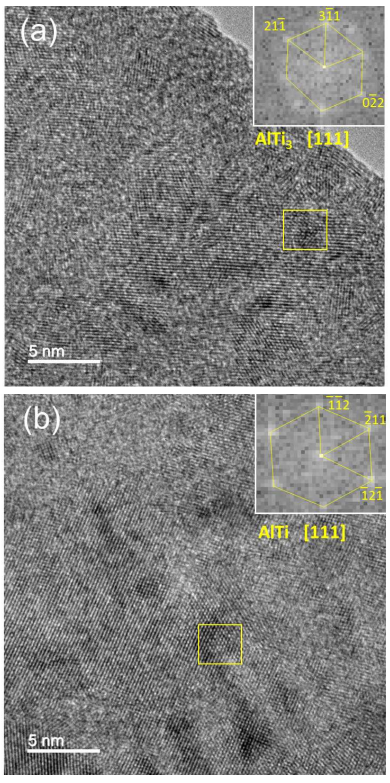

FIG. 3: (Color online) HRTEM images and diffractgrams for Al:Ti:Mg = 1:2:0 subjected to room-temperature HPT for $N = 500$ under $P = 6$ GPa with $\omega = 1.0$ rpm. The intermetallics phases of $AlTi_3$ and AlTi are identified in the square areas in (a) and (b), respectively.

C. Magnetic Measurements

Figure 4 shows the T dependence of M_{AC}' for the sample of Al:Ti:Mg = 1:2:0 subjected to HPT processing through N = 500 at room temperature. The result of N = 100 is included in the inset for comparison. For N = 500, two diamagnetic signals appear at ~10 K and at ~55 K and this is reproducible using two AC measurements with 10 and 100 Hz. These diamagnetic signals disappears by applying H_{DC} as shown in Fig. 5, and the onset temperature in the higher temperature side shows the H_{DC} dependence as seen in the inset of Fig. 5. The results suggest the possibility of superconductivity. In the sample after N = 100, the diamagnetic signal below ~10 K exhibits a double-step anomaly at 3-4 K and ~8 K.

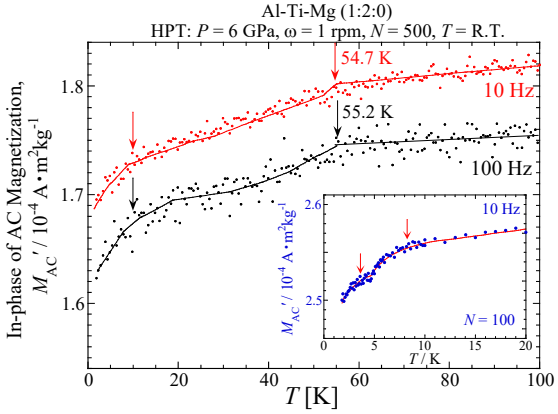

FIG. 4: (Color online) T dependence of M_{AC}' for Al:Ti:Mg = 1:2:0 subjected to room-temperature HPT for N = 500 under P = 6 GPa with ω = 1.0 rpm. The inset shows the results for N = 100.

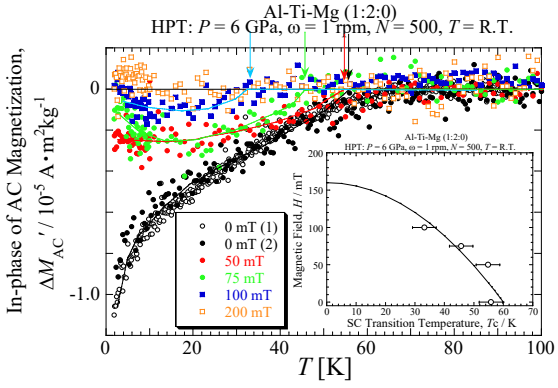

FIG. 5: (Color online) T dependence of M_{AC}' for Al:Ti:Mg = 1:2:0 subjected to room-temperature HPT for N = 500 under P = 6 GPa with ω = 1.0 rpm. Arrows indicate onset temperatures T_c. The inset shows the H_{DC} dependence of T_c, where the best fit line is drawn by $H_{DC} = H_c(0)\{1 - [T/T_c(0)]^2\}$ with $H_c(0)$ = 160 mT and $T_c(0)$ = 60 K.

Figure 6(a) shows the T dependence of M_{AC}' for the composition of Al:Ti:Mg = 1:2:0 after processing by "hot-slow HPT" under P = 6 GPa through N = 10, where the processing temperature was elevated to 573 K and the processing speed was lowered to 0.2 rpm. The T dependence of M_{AC}' includes a background with linear T gradient delineated in red. Thus, the background is subtracted from M_{AC}' and the resultant quantity, $\Delta M_{AC}'$ is also presented as a function of T in blue in Fig. 6(a). The inset in Fig. 6(a) shows enlargement of $\Delta M_{AC}'$ for the T range from 10 to 200 K. The $\Delta M_{AC}'$ below 10 K under several selected values of H_{DC} are presented in Fig. 6(b). Now, the triple-step diamagnetic signal of $\Delta M_{AC}'$ below 10 K, seen at N = 100 in the inset of Fig. 4, becomes much clearer with this hot-slow HPT processing. The anomalies sharply appear at 3, 4, and 7 K and all exhibit the H_{DC} dependence of the onset temperature, which is characteristic of the SC state. Here, we define the onset temperature in $\Delta M_{AC}'$ as the SC transition temperature (T_c). Moreover, as seen in the inset of Fig. 6(a), the anomaly observed at ~55 K after N = 500 in Fig. 4 shifted to a higher T side as at ~93 K in the hot-slow HPT. Figure 7 shows the H_{DC} dependence of T_c's, and the three curves are drawn for $H_{DC} = H_c(0)\{1 - [T/T_c(0)]^2\}$ with $T_c(0)$ and $H_c(0)$ values as (a) (7.3 K, 81 mT), (b) (4.0 K, 24 mT), and (c) (2.8 K, 10 mT). Their analyses thus demonstrate that at least two individual SC states with T_c = 4.0 and 7.3 K are newly stabilized in the disk processed by the hot-slow HPT.

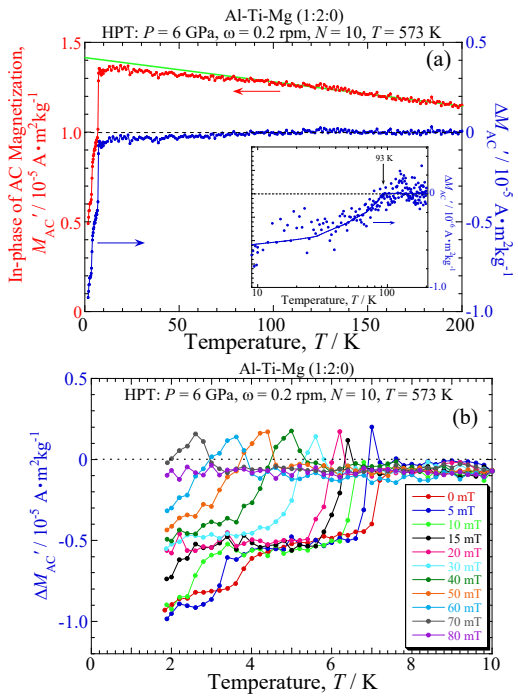

FIG. 6: (Color online) (a) T dependence of M_{AC}' for Al:Ti:Mg = 1:2:0 after processing by HPT at 573 K for N = 10 under P = 6 GPa with ω = 0.2 rpm. $\Delta M_{AC}'$ is the difference after subtracting a linear slope from th total. (b) T dependence of $\Delta M_{AC}'$ at several H_{DC} up to 80 mT.

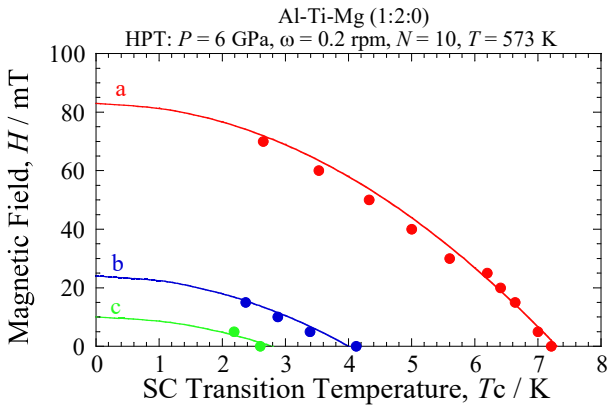

FIG. 7: (Color online) H_{DC} dependence of T_c for Al:Ti:Mg = 1:2:0 subjected to hot-slow HPT. The three curves represent $H_{DC} = H_c(0)\{1 - [T/T_c(0)]^2\}$. From the high T side, the $T_c(0)$ and $H_c(0)$ values are (a) (7.3 K, 81 mT), (b) (4.0 K, 24 mT), and (c) (2.8 K, 10 mT).

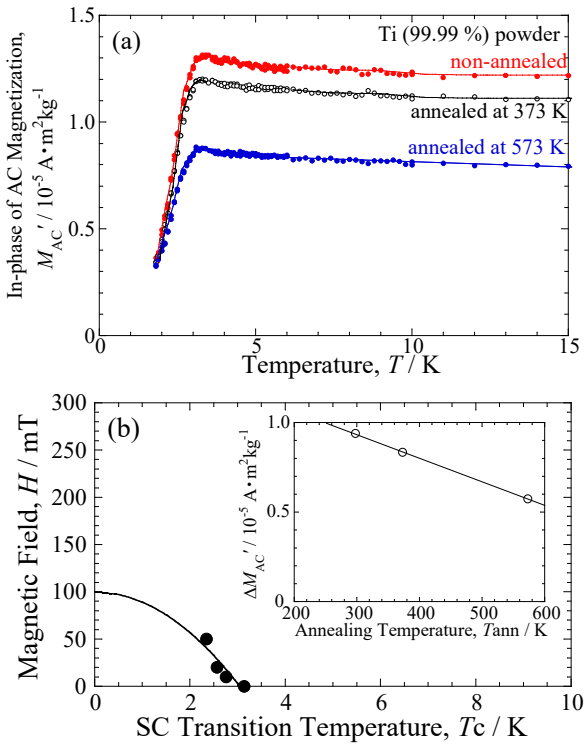

FIG. 8: (Color online) (a) T dependence of M_{AC}' for pure Ti powder (99.9%) and the ones annealed at 373 K and 573 K. (b) H_{dc} dependence of T_c. Solid curve represents $H_{DC} = H_c(0)\{1-[T/T_c(0)]^2\}$ with $T_c(0)$ = 3.05 K and $H_c(0)$ = 100 mT. Inset indicates difference between $M_{AC}'(T_c)$ and M_{AC}'(1.8 K) with respect to annealing temperature (T_{ann}).

V. DISCUSSION

We observed that the pure Ti powder (99.9%) exhibits a weak diamagnetic signal at 3 K as shown in Fig. 8(a). This suggests that the Ti powder originally includes a small amount of an SC domain. As shown in the inset of Fig. 8(b), the magnitude of the SC signal is reduced after annealing. The H_{DC} dependence is described by $H_{DC} = H_c(0)\{1 - [T/T_c(0)]^2\}$ with $T_c(0)$ = 3.05 K and $H_c(0)$ = 100 mT as seen in Fig. 8(b). We confirmed the absence of this SC signal when a pure Ti ingot in a bulk form was examined at the same condition. It is generally known that the efficiency of physisorption of oxygen increases with the surface area. It is probable that the SC signal originates from any Ti-oxides except TiO_2 on Ti powders. Based on a quantitative analysis considering a Ti density of 4.506 g/cm^3 as a standard reference data, the volume fraction of the Ti oxide is estimated to be 0.014 %. Indeed, the fraction is so small that it is quite difficult to determine the SC composition through the X-ray structural analysis. According to Ref. [13], it is most plausible that the Ti-oxide present in the pure Ti powder and the SC signal would be a Magnéli phase with a composition of Ti_4O_7. The $H_c(0)$ value for the anomaly with $T_c(0)$ = 2.8 K in Fig. 7 is much smaller than that for the 3 K anomaly in Fig. 8. However, we consider that the anomaly with $T_c(0)$ = 2.8 K in Fig. 7 is intrinsically the same as the 3 K anomaly in Fig. 8, and the difference of the $H_c(0)$ value would originate from the difference in the grain size.

In this study, the inclusion of an SC Ti-oxide could not be avoided. Nevertheless, this provides an important indication for the formation of a new compound with an SC state if a magnetic anomaly would be observed above 3 K. Specifically, it is suggested that we should include the effect of oxygen on the superconductivity other than the elements of Al, Ti and Mg. Our recent study showed that the composition of Al:Ti:Mg = 1:1:1 led to the formation of several intermetallic phases after HPT processing [27] but the diamagnetic measurement showed the 3 K anomaly. However, the composition of Al:Ti:Mg = 1:2:0 investigated in this study clearly exhibited new diamagnetic signals at 4.0 and 7.3 K which are different from the aforementioned 3 K anomaly. The total magnitude of diamagnetic signals per unit mass is almost consistent with that of the 3 K anomaly.

In Fig. 1, the values of T_c determined experimentally are marked at the compositions with colors corresponding to the color code for the prediction mapping by the machine learning. Although the experimental values of T_c are slightly lower than the predicted using the machine learning, the overall trend is well consistent. The diamagnetic signal at 3 K was already observed in the original Ti powders. The results for the HPT processed Al-Ti-Mg suggest that new SC states exist in the region around Al:Ti = 1:2. Regarding the temperatures above 20 K, a weak diamagnetic signal at 40–50 K was also observed in the compositions of Al:Ti:Mg = 1:2:0 and 1:1:1.

Although all of the AlTi-oxides such as $AlTi_2O_5$ [37] have been reported to be semiconductors, preliminary machine learning for Al-Ti-O based on about 14,000 superconductor dataset [30], including cuprate and iron-based superconductors, predicted high-T_c superconductors with high O concentrations as shown in Fig. 9. In order to avoid overfitting, the data of about 500 non-superconductors reported by Hosono *et al.* [33] have been added to this T_c prediction. In the region with T_c = 20–30 K, there are quasi stable phases with the Al:Ti ratio of 1:1 such as $AlTiO_3$ and $Al_2Ti_2O_7$ [38]. Indeed, in the present experiment, the high T_c was observed in the Al:Ti ratio of 1:2.

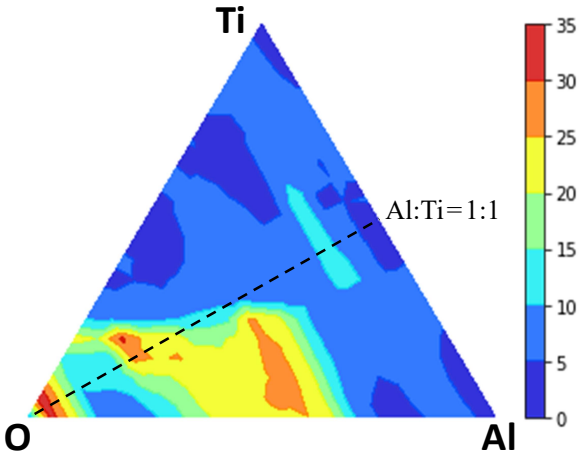

FIG. 9: (Color online) Mapping of T_c in Al-Ti-O ternary system, predicted by machine learning based on about 14,000 superconductor dataset, including cuprate and iron-based superconductors. In order to avoid overfitting by machine learning, the dataset was supplemented with about 500 non-superconductors reported by Hosono *et al.* [33].

It is reasonable to consider that the most promising candidates for the SC states should be the Al-Ti-oxides but their volume fractions must be small in the present HPT-processed samples. The oxides may be in the form of small grains with the sizes of 100 nm or less as the HRTEM analysis in Fig. 3 and as in our earlier report [27]. Alternatively, the oxides may be in a form of thin layers which would be preferentially formed during mechanical contact between Al- and Ti-rich regions. In any forms, the SC regions would be buried in aggregates composed with the non-SC grains. Indeed, their verification by XRD and TEM has not been successfully conducted. Furthermore, it should be noted that the measurements by electrical resistance and/or heat capacity are not applicable to the present samples because the SC magnetic signal is so small that the overlap by paramagnetic signals at the DC magnetic field makes it difficult to detect the the SC signal. Thus, the standard physical approaches are not useful for the verification of the SC states, and this is why the present study employed the AC magnetization measurement under small AC field which is more suitable than the DC measurement. For reference, it should be also noted that an SC signal was not detected when a mixture of TiO_2 and Al_2O_3 was directly processed by HPT. This suggests that the Al-Ti oxides for the SC states should not be synthesized by a dynamical reaction between TiO_2 and Al_2O_3 but requires a condition where Al and Ti are highly strained in mutual contact by HPT processing under an oxygen atmosphere.

Herein, we deduce that the superconductor in the present HPT-processed material would be a non-stoichiometric phase like a Magnéli phase characterized as Ti_nO_{2n-1} (n = 3-10). The Magnéli phase is a non-stoichiometric phase with the O/Ti ratio of more than 1.6 [39], and it is constructed by inserting Ti_2O_3 to TiO_2. Recently in the sulfur hydride with T_c of above 200 K, the importance of Magnéli phase has theoretically been suggested [40]. Indeed, Ti_4O_7 discussed in association with Fig. 8 also belongs to the Magnéli phase [41]. In the present Al-Ti-O superconductor, the valence of Ti would deviate from +4. For instance, Ti of $AlTi_2O_5$ has the non-formal valence of +3.5 that is the same as the situation in the Magnéli compound Ti_4O_7. Generally, the stabilization of the Magnéli phase requires the delicate condition of temperature and oxide pressure [42–45]. Thus, it is difficult to produce the non-stoichiometric SC oxides in the Al-Ti-O system by thermal energy ΔQ alone. Therefore, the input of mechanical energy ΔW by HPT process becomes important. We emphasize that the HPT processing could be effective to produce a non-stoichiometric charge state. The key approach to increase the volume fraction of the SC oxides is to optimize the conditions of the HPT processing such as temperature, pressure, and imposed strain as well as the conditions of starting materials as powder sizes and total compositions.

The stabilization of the Magnéli-like compound is equivalent to the condition that the electrons are doped into the Ti-oxide. If the antiferromagnetic correlation would develop in the AlTi oxide like cuprate superconductors, the phenomenological situation became similar to the electron-doped cuprate superconductors.

Finally, we should comment another scenario for the origin of the diamagnetic signal at around 50-60 and 90 K. If the Al-Ti-O material would be a low-dimensional magnetic oxide, there could occur the spin-dimerization accompanying the structural change as reported in $CuGeO_3$ [46, 47] and NaV_2O_5 [48], for example. However, the present Al:Ti = 1:2 specimen exhibits no broad hump characteristic of the antiferromagnetic short-range order. It is not reasonable to consider the present Al:Ti = 1:2 specimen as any magnetic system. Consequently, as only a possible scenario, there remains only the possibility of magnetic shielding effect characteristic of superconductivity.

VI. CONCLUSIONS

In this study, we successfully synthesized new superconductors based on the prediction by machine learning for three lightweight metallic elements—Al, Ti and Mg—and by consolidating powder mixtures using the HPT process. AC magnetic anomalies clearly appeared at 4.0 and 7.3 K with magnetic shielding effects when the HPT processing was performed at 573 K on a powder mixture of Al:Ti = 1:2. The magnetic anomalies also appeared at ∼55 K and ∼93 K, and this is consistent with the machine learning-based predictions, which included the effect of oxygen. This suggests that Al-Ti oxides play an important role in the advent of such anomalies. The addition of Mg could be less effective to stabilize a superconducting state.

Acknowledgments

This work was supported by the Light Metals Educational Foundation of Japan. The synchrotron radiation experiments were performed at the BL04B1 of SPring-8 with the approval of the Japan Synchrotron Radiation Research Institute (JASRI) (Proposal No. 2019B1496).

Author Declarations

Conflict of Interest

The author has no conflicts to disclose.

Data Availability

The data that support the findings of this study are available from the corresponding author upon reasonable request.

[1] J. J. Hamlin, Physica C (Amsterdam, Neth.) **514**, 59 (2015).
[2] M. Mito, H. Kondo, T. Arase, K. Irie, S. Takagi, H. Deguchi, T. Tajiri, and M. Ishizuka, Phys. Rev. B **104**, 054431 (2021).
[3] B. T. Matthias, T. H. Geballe, and V. B. Compton, Rev. Mod. Phys. **35**, 1 (1963).
[4] L. Shumei, Z. Dianlin, J. Xiunian, L. Li, L. Shanlin, K. Ning, W. Xiaosong, and J. J. Lin, Phys. Rev. B **62**, 8695 (2000).
[5] E. M. Savitskii, V. V. Baron, Y. V. Efimov, M. I. Bychkova, and L. F. Myzenkova, *Superconducting Materials* (Springer, Boston, 1973).
[6] T. Claeson, Physica Scripta **9**, 353 (1974).
[7] E. Bauer, H. Kaldarar, R. Lackner, H. Michor, W. Steiner, E. W. Scheidt, A. Galatanu, F. Marabelli, T. Wazumi, K. Kumagai, et al., Phys. Rev. B **76**, 014528 (2007).
[8] C. G. Granqvist, J. Ivarsson, and T. Claeson, Phys. Stat. Sol. **60**, 157 (1973).
[9] N. J. Doyle, J. K. Hulm, C. K. Jones, R. C. Miller, and A. Taylor, Phys. Lett. A **26**, 604 (1968).
[10] J. K. Hulm, C. K. J. J. K. Hulm, and C. K. Jones, J. Low. Temp. Phys. **7**, 291 (1972).
[11] T. B. Reed, M. D. Banus, M. Sjöstrand, and P. H. Keesom, J. Appl. Phys. **43**, 2478 (1972).
[12] C. Zhang, F. Hao, G. Gao, X. Liu, C. Ma, Y. Lin, Y. Yin, and X. Li, npj Quantum Materials **2**, 2 (2017).
[13] K. Yoshimatsu, O. Sakata, and A. Ohtomo, Sci. Rep. **7**, 12544 (2017).
[14] S. Sekiguchi, T. Shiraishi, K. Miura, C. Kawashima, K. Yoshimatsu, A. Ohtomo, H. Kamioka, and H. Takahashi, J. Phys. Soc. Jpn. **88**, 035001 (2019).
[15] W. Hu, Z. Feng, B.-C. Gong, G. He, D. Li, M. Qin, Y. Shi, Q. Li, Q. Zhang, J. Yuan, et al., Phys. Rev. B **101**, 220510(R) (2020).
[16] K. Matsumoto and T. Horide, Appl. Phys. Express. **12**, 073003 (2019).
[17] R. Matsumoto, Z. Hou, M. Nagao, S. Adachi, H. Hara, H. Tanaka, K. Nakamura, R. Murakami, S. Yamamoto, H. Takeya, et al., Sci. Technol. Adv. Mater. **19**, 909 (2018).
[18] R. Matsumoto, Z. Hou, S. Adachi, M. Nagao, S. Yamamoto, P. Song, N. Kataoka, P. B. de Castro, K. Terashima, H. Takeya, et al., High Pressure Res. **40**, 22 (2020).
[19] P. W. Bridgman, Phys. Rev. **48**, 825 (1935).
[20] R. Valiev, Y. Estrin, Z. Horita, T. Langdon, M. Zehetbauer, and Y. Zhu, JOM **58**, 33 (2006).
[21] M. Mito, H. Matsui, K. Tsuruta, T. Yamaguchi, K. Nakamura, H. Deguchi, N. Shirakawa, H. Adachi, T. Yamasaki, H. Iwaoka, et al., Sci. Rep. **6**, 36337 (2016).
[22] H. Razavi-Khosroshah and M. Fuji, Mater. Trans. **60**, 1203 (2019).
[23] Y. Ikoma, Mater. Trans. **60**, 1168 (2019).
[24] M. Mito, S. Shigeoka, H. Kondo, N. Noumi, Y. Kitamura, K. Irie, K. Nakamura, S. Takagi, H. Deguchi, T. Tajiri, et al., Mater. Trans. **60**, 1472 (2019).
[25] T. Nishizaki, K. Edalati, S. Lee, Z. Horita, T. Akune, T. Nojima, S. Iguchi, and T. Sasaki, Mater. Trans. **60**, 1367 (2019).
[26] A. Bachmaier and R. Pippan, Mater. Trans. **60**, 1256 (2019).
[27] Y. Tang, M. Murayama, K. Edalati, Q. Wang, S. Iikubo, T. Masuda, Y. Higo, Y. Tange, Y. Ohishi, M. Mito, et al., J. Alloys Comp. **889**, 161815 (2021).
[28] K. Edalati and Z. Horita, Rev. Adv. Mater. Sci. **31**, 5 (2012).
[29] Z. Horita, Y. Tang, T. Masuda, and Y. Takizawa, Mater. Trans. **61**, 1177 (2020).
[30] *Database of Superconductors*

(http://supercon.nims.go.jp/).
[31] G. Garbarino and M. Núñez-Regueiro, Solid State Commun. **142**, 306 (2007).
[32] J. Nagamatsu, N. Nakagawa, T. Muranaka, Y. Zenitani, and J. Akimitsu, Nature **410**, 63 (2000).
[33] H. Hosono, K. Tanabe, E. Takayama-Muromachi, H. Kageyama, S. Yamanaka, H. Kumakura, M. Nohara, H. Hiramatsu, and S. Fujitsu, Sci. Technol. Adv. Mater. **16**, 033503 (2015).
[34] Z. Horita, D. Maruno, Y. Ikeda, T. Masuda, Y. Tang, M. Arita, Y. Higo, Y. Tange, and Y. Ohishi, Mater. Trans. **62**, 167 (2020).
[35] K. Edalati, Mater. Trans. **60**, 1221 (2019).
[36] A. Mazilkin, B. Straumal, A. Kilmametov, P. Straumal, and B. Baretzky, Mater. Trans. **60**, 1489 (2019).
[37] T. Tohyama, R. Ogura, K. Yoshinaga, S. Naito, N. Miyakawa, and E. Kaneshita, J. Phys. Chem. Solid **127**, 252 (2019).
[38] *The Materials Project* (https://materialsproject.org/).
[39] S. Andersson and A. Magnéli, Die Naturwissenschaften **43**, 495496 (1956).
[40] R. Akashi, W. Sano, R. Arita, and S. Tsuneyuki, Phys. Rev. Lett. **117**, 075503 (2016).
[41] A. F. Arif, R. Balgis, T. Ogi, F. Iskandar, A. Kinoshita, K. Nakamura, and K. Okuyama, Sci. Rep. **7**, 3646 (2017).
[42] N. J. Bogdanova, G. P. Pirogorskaya, and S. M. Ariya, Zh. Neorg. Khim. **8**, 785 (1963).
[43] P. W. Gilles, K. D. Carlson, H. F. Franzen, and P. G. Wahlbeck, J. Chem. Phys. **46**, 2461 (1967).
[44] Y.-B. Kang and H.-G. Lee, ISIJ Int. **45**, 1543 (2005).
[45] Y.-B. Kang, I.-H. Jung, and H.-G. Lee, Computer Coupling of Phase Diagrams and Thermochemistry **30**, 235247 (2006).
[46] M. Hase, I. Terasaki, and K. Uchinokura, Phys. Rev. Lett. **70**, 3651 (1993).
[47] K.Hirota, D. E. Cox, I. .E.Lorenzo, G. Shirane, I. M. Tranquada, M. Hase, K. Uchinokura, H. Kojima, and Y. S. and.Tanaka, Phys. Rev. Lett. **73**, 736 (1994).
[48] M. Isobe and Y. Ueda, J. Phys. Soc. Jpn. **65**, 1178 (1996).